broadens, due to thermal excitation, faster than the increase of the Fermi level, until the Fermi level is below the band top and holes are formed in the 7s band leading to a positive Hall coefficient. This is shown schematically in Fig. 4.

ACKNOWLEDGMENT

The author wishes to thank N. Griffin for his assistance in carrying out the measurements. The encouragement and suggestions of L. T. Lloyd are gratefully acknowledged.

PHYSICAL REVIEW VOLUME 131, NUMBER 1 1 JULY 1963

Superconductivity at High Magnetic Fields*

T. G. Berlincourt and R. R. Hake
Atomics International Division of North American Aviation, Inc., Canoga Park, California
(Received 6 February 1963)

Using pulsed-magnetic-field techniques, we have studied the magnetic-field-induced superconducting transitions of alloys in the systems Ti-V, Ti-Nb, Ti-Ta, Ti-Mo, Zr-Nb, Hf-Nb, Hf-Ta, U-Nb, and U-Mo. For concentrated alloys the low-current-density resistive critical field $H_r(J \lesssim 10\ \mathrm{A/cm^2})$ is nearly independent of the amount of cold working and the relative orientations of magnetic field, current, and anisotropic defect structure. The observed values of $H_r(J=10)$ peak up sharply (reaching 145 kG in the Ti-Nb system) in the vicinity of ~4.5 "valence" electrons per atom, an electron concentration where peaking also typically occurs for such (approximately) defect-independent transition metal alloy parameters as superconducting transition temperature, thermodynamic critical field, and electronic specific heat coefficient. All the above evidence suggests that in these alloys $H_r(J=10)$ is determined principally by bulk electronic parameters, rather than by the nature of extended lattice defects. This view is further supported by the observation that, for several Group V-rich, Group IV–Group V transition metal alloys, excellent quantitative agreement is achieved in adjustable-parameter-free comparisons of $H_r(J=10)$ with H_{c2}, the "upper critical field" predicted on the basis of bulk electronic parameters by the Ginzburg-Landau-Abrikosov-Gor'kov (GLAG) theory for the case of negative surface energy. For certain ranges of alloy composition, it appears that normal-state paramagnetic free-energy considerations, ignored in the GLAG theory, impose limitations on $H_r(J=10)$ in good accord with the theoretical predictions of Clogston. Additional experimental results are reviewed, and it is argued that a comprehensive theoretical understanding of high-field superconductivity in bulk materials may be achieved on the basis of the GLAG theory, modified to include paramagnetic free-energy terms, and extended to consider transport supercurrents stabilized in a manner similar to that suggested by Gorter and Anderson. The *a priori* assumptions of Mendelssohn's filamentary-mesh model appear, on the other hand, to be inadequate for a suitable description.

I. INTRODUCTION

RECENT progress in the understanding and characterization of high-magnetic-field superconductors has been particularly rapid, and the broad outlines of a reasonable picture appear already to have been established. Significant differences exist between this picture and the earliest model. The latter, hereafter referred to as the filamentary-mesh model, hypothesized a multiply connected high-critical-field filamentary network embedded in a matrix of low-critical-field material.[1] The high critical fields of the filaments followed either from chemical or physical inhomogeneity[1] directly or (on simple thermodynamic arguments) from the small filament dimensions,[2–5] i.e., any observed filamentary critical field could be rationalized by the assumption of a suitable filament diameter. Such ideas have recently been widely assumed to account satisfactorily for most properties of high-magnetic-field superconductors.[3–7] However, for reasons to be discussed at length below, an alternative (and more general) interpretation of high-field superconductivity is gaining wide acceptance. In this alternative picture, the main bulk of a high-field superconductor remains superconducting up to an "upper critical field" determined by bulk (or nonfilamentary) electronic parameters, essentially as predicted by the "homogeneous" Ginzburg-Landau-Abrikosov-Gor'kov (GLAG) theory.[8–11] In certain cases,[12] the upper critical field may be limited as predicted by Clogston[13]

* This research was supported by the U. S. Atomic Energy Commission.

[1] K. Mendelssohn, Proc. Roy. Soc. (London) A152, 34 (1935).
[2] C. J. Gorter, Physica 2, 449 (1935).
[3] J. E. Kunzler, Rev. Mod. Phys. 33, 501 (1961).
[4] J. J. Hauser and E. Buehler, Phys. Rev. 125, 142 (1962).
[5] J. J. Hauser and E. Helfand, Phys. Rev. 127, 386 (1962).
[6] C. P. Bean, Phys. Rev. Letters 8, 250 (1962).
[7] R. D. Blaugher and J. K. Hulm, Phys. Rev. 125, 474 (1962).
[8] V. L. Ginzburg and L. D. Landau, Zh. Exsperim. i Teor.Fiz 20, 1064 (1950); V. L. Ginzburg, Nuovo Cimento 2, 1234 (1955).
[9] A. A. Abrikosov, Zh. Exsperim. i Teor. Fiz. 32, 1442 (1957) [translation: Soviet Phys.—JETP 5, 1174 (1957)].
[10] L. P. Gor'kov, Zh. Eksperim. i Teor. Fiz. 37, 1407 (1959) [translation: Soviet Phys.—JETP 10, 998 (1960)].
[11] L. P. Gor'kov, Zh. Eksperim. i. Teor. Fiz. 37, 835 (1959) [translation: Soviet Phys.—JETP 10, 593 (1960)].
[12] T. G. Berlincourt and R. R. Hake, Phys. Rev. Letters 9, 293 (1962).
[13] A. M. Clogston, Phys. Rev. Letters 9, 266 (1962).

and Chandrasekhar[14] by normal-state paramagnetic energy considerations ignored in the GLAG formulation. However, in both instances the upper critical field is virtually independent of extended lattice inhomogeneities, and *bulk* superconductivity may exist at fields well above 100 kG even in perfect single crystals, provided their bulk electronic parameters fulfill certain criteria. This high-field superconducting state can be destroyed by application of a critical transport current density, presumably a consequence, in part, of Lorentz forces. Unlike the upper critical field, the critical current density is very sensitive to the extent and nature of lattice defects and inhomogeneities.[15–18] Gorter[19,20] and Anderson[21] have pointed out that inhomogeneities may be expected to provide free-energy barriers which may counter the deleterious action of the Lorentz force on the high-field superconducting state.

The relevance of the GLAG theory to the persistance of superconductivity at very high magnetic fields has been stressed by Goodman[22,23] and the present authors.[12,17,18,24–26] In the latter references, we established the low-current-density resistive critical field as an experimental quantity which for concentrated alloys appears to depend principally on the bulk electronic parameters of importance in the GLAG theory and to be virtually independent of the degree of cold working and the relative orientations of magnetic field, current, and defect structure. Indeed, for several transition-metal alloys excellent accord was noted[12,17,24–26] between experimental low-current-density resistive critical fields and (1) upper critical fields predicted by the GLAG theory, or (2) limiting critical fields calculated according to Clogston's criterion.[13] It is particularly significant that this agreement was obtained *without adjustable parameters*.

In this paper, detailed pulsed-magnetic-field data on upper critical fields and normal-state electrical resistivities are reported for a number of transition-metal alloys in the systems Ti-V, Ti-Nb, Ti-Ta, Ti-Mo, Zr-Nb, Hf-Nb, Hf-Ta, U-Nb, and U-Mo. Comparisons of these data with the predictions of GLAG and Clogston are carried out in more detail than in our earlier work. Other experimental results which bear on the GLAG and filamentary-mesh pictures are briefly reviewed, and transport supercurrent effects are considered with reference to inhomogeneities and the Gorter-Anderson[19–21] supercurrent stabilization mechanism. It is concluded that (1) several difficulties exist in attempts to utilize the filamentary-mesh model as a foundation for understanding high-field superconductivity, and (2) a more realistic general characterization of high-field superconductors may be achieved on the basis of the GLAG theory, modified to include Clogston-type normal-state paramagnetic free-energy terms, and extended to consider transport supercurrents stabilized in a manner similar to that hypothesized by Gorter and Anderson.

II. THEORETICAL BACKGROUND

A. The GLAG Theory

According to the Ginzburg-Landau theory,[8] superconductors may be broadly classified[9] on the basis of a parameter κ which is approximately[22] equal to $\lambda_L(0)/\xi$, where $\lambda_L(0)$ is the London penetration depth at absolute zero and ξ is the superconducting-state coherence distance. For $\kappa<1/\sqrt{2}$, the supernormal surface energy is positive, and the superconductor is said to be "of the first kind." For a bulk superconductor of the first kind having a negligible demagnetizing coefficient and a negligible normal-state magnetic free energy, a complete Meissner effect[27] (magnetic flux confined to a thin surface layer of thickness comparable to the London penetration depth) is observed up to the "thermodynamic critical field"

$$H_c\approx H_0[1-(T/T_c)^2]\approx 2.42\gamma^{1/2}T_c[1-(T/T_c)^2], \quad (1)$$

where H_0 is the thermodynamic critical field at $T=0$, T_c is the superconducting transition temperature, γ is the electronic specific heat coefficient per unit volume [proportional to the electronic density of states at the Fermi level $N(0)$], and the BCS[28] relation $\gamma T_c^2/H_0^2\approx 0.17$ has been used. The normal state is restored at H_c, and complete magnetic-flux penetration takes place abruptly. Furthermore, for a bulk superconductor of the first kind, the supernormal transition is second order in zero magnetic field and first order in the presence of a field. Throughout this paper we retain the usual definition of the thermodynamic critical field such that the zero-field free-energy difference per unit volume between the normal and superconducitng states (condensation energy) is given by

$$G_N(0)-G_S(0)\equiv H_c^2/8\pi\approx 0.234\gamma T_c^2[1-(T/T_c)^2]^2. \quad (2)$$

[14] B. S. Chandrasekhar, Appl. Phys. Letters **1**, 7 (1962).
[15] T. G. Berlincourt, R. R. Hake, and D. H. Leslie, Phys. Rev. Letters **6**, 671 (1961).
[16] R. R. Hake, T. G. Berlincourt, and D. H. Leslie, IBM J. Res. Develop. **6**, 119 (1962).
[17] R. R. Hake and D. H. Leslie, J. Appl. Phys. **34**, 270 (1963).
[18] R. R. Hake, D. H. Leslie, and C. G. Rhodes, in *Proceedings of the Eighth International Conference on Low-Temperature Physics* [Butterworths Scientific Publications Ltd., London (to be published)].
[19] C. J. Gorter, Phys. Letters **2**, 26 (1962).
[20] C. J. Gorter, in *Proceedings of the Eighth International Conference on Low-Temperature Physics* [Butterworths Scientific Publications Ltd., London (to be published)].
[21] P. W. Anderson, Phys. Rev. Letters **9**, 309 (1962).
[22] B. B. Goodman, IBM J. Res. Develop. **6**, 63 (1962).
[23] B. B. Goodman, Phys. Letters **1**, 215 (1962).
[24] T. G. Berlincourt and R. R. Hake, postdeadline paper, Washington Meeting, Bull. Am. Phys. Soc. (1962) (unpublished).
[25] T. G. Berlincourt and R. R. Hake, Bull. Am. Phys. Soc. **7**, 408 (1962).
[26] T. G. Berlincourt, in *Proceedings of the Eighth International Conference on Low-Temperature Physics* [Butterworths Scientific Publications Ltd., London (to be published)].
[27] For a discussion of the Meissner effect see D. Shoenberg, *Superconductivity* (Cambridge University Press, Cambridge, 1952), p. 13 ff.
[28] J. Bardeen, L. N. Cooper, and J. R. Schrieffer, Phys. Rev. **108**, 1175 (1957).

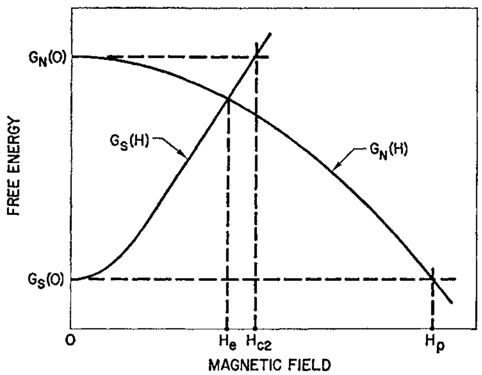

FIG. 1. Schematic representation of the magnetic-field dependence of the free energies of the normal-state and the high-field superconducting state illustrating the meanings of the fields H_{c2} and H_p and indicating that H_e, the experimental upper critical field, should be less than the smaller of H_{c2} and H_p.

If $\kappa > 1/\sqrt{2}$, the interphase surface energy is negative,[29] and the superconductor is said to be "of the second kind." Abrikosov's theory[9] for a *perfectly homogeneous* superconductor of the second kind yields a reversible magnetization curve characterized by a complete Meissner effect for fields up to a "lower critical field" H_{c1}.[30] For $\kappa \gg 1$, H_{c1} is given by

$$H_{c1} = (H_c/\sqrt{2}\kappa)(\ln\kappa + 0.08), \qquad (3)$$

while for smaller κ values H_{c1} may be obtained from Goodman's interpolation[22] of Abrikosov's theory. As the applied field is increased above H_{c1}, the flux gradually penetrates forming a "mixed state" comprised of a lattice-like array of dissipationless, quantized, flux-enclosing, supercurrent vortices extending throughout the sample. It is important to emphasize that the main bulk of the sample remains in the superconducting state during this field penetration, the position-dependent superconducting order parameter (later related by Gor'kov[31] to the BCS energy gap) vanishing, according to Abrikosov, only along a (zero volume) line at the center of each vortex.[32] Simply stated, above H_{c1} it is energetically less costly for the specimen to establish flux-enclosing supercurrent vortices (with modest reduction of the average energy gap) than (1) to establish penetration-depth shielding currents of the magnitude required for a complete Meissner effect (and preservation of the zero-field energy gap), or (2) to create regions of the higher energy normal material through which the flux may penetrate to relieve the Maxwell pressure. This particular energy balance is a consequence of the negative interphase surface energy as determined by the relative magnitudes of the penetration depth and coherence distance.[29] In any event, according to Abrikosov,[9,30] the mixed state, or high-field superconducting state, persists to an "upper critical field" given by

$$H_{c2} = \sqrt{2}\kappa H_c, \qquad (4)$$

where flux penetration is complete, and a *second-order* transition to the normal state occurs. Although Abrikosov presented arguments suggesting that Eq. (4) should be valid for all $T < T_c$, Gor'kov[11] and Shapoval[33] have asserted that H_{c2}/H_c should be temperature-dependent. According to Gor'kov[11]

$$H_{c2} = [1.77 - 0.43(T/T_c)^2 + 0.07(T/T_c)^4]\kappa H_c, \qquad (5)$$

whereas Shapoval[33] predicts a nearly linear temperature dependence between the end points

$$H_{c2} = 3.03\kappa H_c, \quad (T=0), \qquad (6)$$
$$H_{c2} = \sqrt{2}\kappa H_c, \quad (T=T_c),$$

with steep slope at $T=0$. It will be convenient in what follows to represent the coefficients of κH_c in Eqs. (4)–(6) by a more general (temperature-dependent) symbol $A(T)$.

It should be noted that H_c (appearing in all the foregoing equations) is related in different ways to the super-normal transition field for the two classifications of superconductors. Nevertheless, H_c may be calculated in

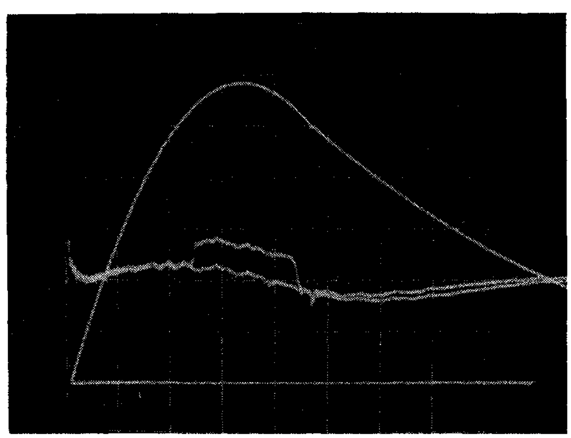

FIG. 2. Oscilloscope recording of magnetic-field-induced resistive transitions for Ti-28.7 V at 1.2°K with $H \perp J$ and $H \parallel RP$. The wiggly traces represent the signal (1 mV/cm) on the potential probes for two successive (and indistinguishable) magnetic-field pulses with and without a measuring current density of $J=10$ A/cm². The magnetic field is shown rising from zero to 107 kG in 6.6 msec.

[29] The surface energy, penetration depth, and coherence distance are elegantly discussed by A. B. Pippard, Proc. Cambridge Phil. Soc. **47**, 617 (1951); Proc. Roy. Soc. (London) **A216**, 547 (1953).

[30] Following Abrikosov (reference 9), we use H_{c1} and H_{c2}, respectively, to designate the lower and upper critical fields. These subscripts are interchanged in a number of later papers by other authors.

[31] L. P. Gor'kov, Zh. Eksperim. i. Teor. Fiz. **36**, 1918 (1959) [translation: Soviet Phys.—JETP **9**, 1364 (1959)].

[32] In discussing the possible existence of supercurrent vortices in simply connected superconductors, A. Bohr and B. R. Mottelson [Phys. Rev. **125**, 495 (1962)] suggest that under certain conditions a small, but nevertheless finite, volume of material at the center of a supercurrent vortex may be normal.

[33] E. A. Shapoval, Zh. Eksperim. i Teor. Fiz. **41**, 877 (1961) [translation: Soviet Phys.—JETP **14**, 628 (1962)].

both cases in terms of γ and T_c. Alternatively, if the normal-state free energy is independent of magnetic field strength, and the superconducting state magnetization curve is reversible, H_c may be deduced from the area under the magnetization curve, which in this case is equal to $G_N(0)-G_S(0)$ [see Eq. (2)] for both first and second group superconductors.

A general expression for κ (applicable to pure metals and alloys) has been obtained by Gor'kov in terms of measurable parameters.[10] Consistent with an expression (analogous to that of Pippard[29]) for the coherence distance, $\xi^{-1}=\xi_0^{-1}+(\alpha' l)^{-1}$ (where ξ_0 is the BCS coherence distance,[28] l is the electron mean free path, and $\alpha'=1.32$), Goodman[22] has approximated $\kappa\sim\lambda_L(0)/\xi$ as the sum of two limiting forms of κ obtained by Gor'kov, viz.,

$$\kappa=\kappa_0+\kappa_l. \tag{7}$$

The first term on the right involves only the electronic structure of the metal, independent of electronic scattering, and is given according to Gor'kov[10,31] by

$$\kappa_0=2a\pi\{6/[7\zeta(3)]\}^{1/2}\lambda_L(0)/\xi_0=0.96\lambda_L(0)/\xi_0, \tag{8}$$

where $a=0.18$ and $\zeta(3)=1.202$. The London penetration depth at absolute zero $\lambda_L(0)$ and the BCS coherence length ξ_0 may be estimated from the expressions[28,34]

$$\lambda_L(0)=(3h^3\gamma^{1/2})/(4\pi^{3/2}ekS) \tag{9}$$

and

$$\xi_0=(a\pi kS)/(3h^2T_c\gamma), \tag{10}$$

where S is the free area of the Fermi surface (in momentum space), h is Planck's constant, k is Boltzmann's constant, and e is the electronic charge in emu. In a more convenient form for comparison with experiment, κ_0 may be expressed as

$$\kappa_0=1.61\times10^{24}(T_c\gamma^{3/2}/n^{4/3})(S_f/S)^2, \tag{11}$$

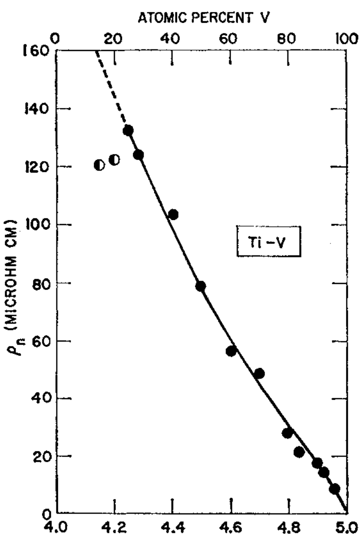

FIG. 3. Normal-state resistivity vs composition and electron concentration for Ti-V alloys at 1.2°K. The half-shaded points represent samples comprised of more than one phase. The deviations of these points from the extrapolated curve enable rough estimates to be made of the amount of second-phase material present.

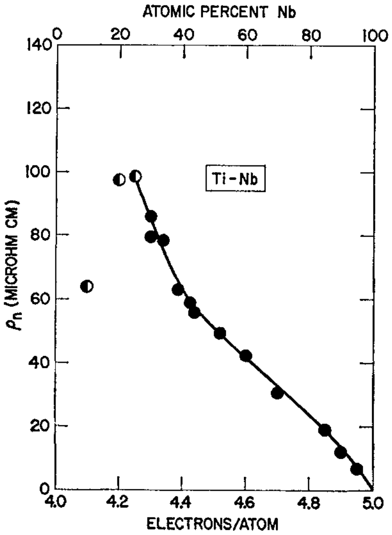

FIG. 4. Normal-state resistivity vs composition and electron concentration for Ti-Nb alloys at 1.2°K. The half-shaded points represent samples comprised of more than one phase.

where n is the average number of "valence" electrons (number of electrons outside closed shells) per unit volume and S_f is the area of the Fermi surface for a free-electron gas of density n.

The second term on the right side of Eq. (7) involves the electron mean free path and is given by Gor'kov[10] as

$$\kappa_l=[21\zeta(3)/2\pi]^{1/2}(e\rho_n\gamma^{1/2}/\pi^3k), \tag{12}$$

where ρ_n, the normal state electrical resistivity, is given in emu. For concentrated alloys in which $\xi\approx l\ll\xi_0$, it follows that $\kappa_l\gg\kappa_0$ and $\kappa\approx\kappa_l$. For this case, combining Eqs. (1) and (12) with Eqs. (4), (5), or (6) yields[35]

$$H_{c2}\approx2.42A(T)[21\zeta(3)/2\pi]^{1/2}\times(e/\pi^3k)\rho_n\gamma T_c[1-(T/T_c)^2], \tag{13}$$

where, as already mentioned, $A(T)$ may be considered as replacing any one of the coefficients of κH_c in Eqs. (4)–(6). It is particularly noteworthy that, aside from the question regarding the form of $A(T)$, H_{c2} is given purely in terms of constants of nature and measurable parameters. Hence, comparison with experiment may be accomplished without adjustable parameters and subject only to an uncertainty in $A(T)$ not exceeding a factor of 2. Furthermore, it follows from the usual association of large ρ_n, γ, and T_c with large $N(0)$ (the magnitude of the electronic density of states at the Fermi level) that large values of H_{c2} are to be anticipated for materials with large $N(0)$.

Other fundamental negative surface energy approaches to the problem of superconductivity in fields greater than H_c have been considered by Pippard,[36]

[34] T. E. Faber and A. B. Pippard, Proc. Roy. Soc. (London) **A231**, 336 (1955).

[35] If ρ_n is expressed in Ω cm, the coefficient of $\rho_n\gamma T_c[1-(T/T_c)^2]$ in Eq. (13) becomes 18 300 $A(T)$.

[36] A. B. Pippard, Phil. Trans. Roy. Soc. (London) **A248**, 97 (1955); also see reference 29.

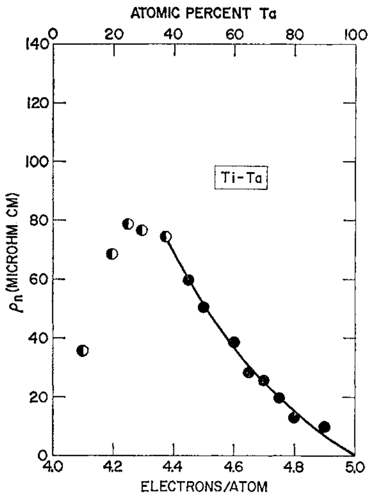

FIG. 5. Normal-state resistivity vs composition and electron concentration for Ti-Ta alloys at 1.2°K. The half-shaded points represent samples comprised of more than one phase.

Doidge,[37] Goodman,[38] and Parmenter,[39] and other supercurrent vortex ideas have been advanced by Bohr and Mottleson,[32] Glick and Ferrell,[40] Yntema,[41] and Tinkham.[42] Although none of these theories permits such an unambiguous, adjustable-parameter-free comparison with so many experimental features, it is, nevertheless, of interest that Doidge's expression [his Eqs. (21) and (22)] for the field which quenches the last remnant of superconductivity is almost equivalent to that given by the GLAG theory. This near equivalence is not surprising in view of the fact that Doidge's derivation is based on the same type of free-energy expansion used by Ginzburg and Landau, and further that the limiting dimension for the last remnant of superconducting material was assumed to be of the order of the coherence length.

A final relevant point regarding the GLAG theory is the fact that for $\lambda_L(T)\gg\xi$ Gor'kov[10,31] has shown that the local Ginzburg-Landau equations can be derived from the BCS theory provided (as in the foregoing equations) proper account is taken of the double charge of the Cooper pair.

B. Clogston's Criterion

As noted by Pippard and Heine[43] the energy gain $2\,\mu_B H$ (where μ_B is the Bohr magneton) resulting from electron-spin alignment along H should become comparable with the opposite-spin-paired superconducting state gap energy $2\epsilon_0\approx 3.5kT_c$ in fields of the order of 100 kG. That this circumstance might impose a limitation on high-field superconductors was recognized independently by Chandrasekhar[14] and Clogston[13] with reference to the filamentary-mesh model. Indeed, Clogston suggested that an *upper limit* H_p to the field at which superconductivity can exist may be estimated[13,44] by equating the Pauli paramagnetic energy $\chi_p H_p^2/2=\mu_B^2 N(0)H_p^2$ to the zero-field energy difference, Eq. (2), between the normal and superconducting states. This is equivalent to assuming that the difference between the *total* susceptibilities of the normal and superconducting states is just the Pauli susceptibility χ_p, an assumption which leads to the relation

$$H_p=(\epsilon_0/\sqrt{2}\mu_B)[1-(T/T_c)^2]$$
$$=18\,400T_c[1-(T/T_c)^2]. \quad (14)$$

TABLE I. Values for ρ_n and $H_r(J=10,\ T=1.2)$ for Ti-V alloys.

At.% V	Reduction ratio	ρ_n ($\mu\Omega$ cm)	$H_r(J=10,\ T=1.2)$ (kG)	
15.0[a]	12.7	120.5	33.9	44.5
20.0[a]	14.1	122.2	53.0	58.7
25.0	17.5	132.5	86.2	87.8
28.7	23.4	124.0	96.3	97.3
40.5	13.7	103.5	109.6	111.4
50.0	16.3	78.9	110.6	112.0
60.0	14.7	56.4	103.0	103.8
70.0	16.7	48.8	94.3	96.2
80.0	38.6	28.0	79.6	81.9
84.0	14.3	21.5	66.0	67.3
90.0	12.3	17.6	48.0	50.8
92.0	13.0	14.5	40.0	43.1
96.0	12.7	8.5	22.3	27.0

[a] Mainly bcc but contained small amount of second phase.

Furthermore, according to Clogston's treatment, the transition at H_p is of first order (in contrast to the second-order transition predicted by GLAG at H_{c2}). It should be noted that when the normal-state magnetic free energy is important the area under the (reversible) magnetization curve is no longer given by $H_c^2/8\pi$ if H_c is defined as in Eq. (2).

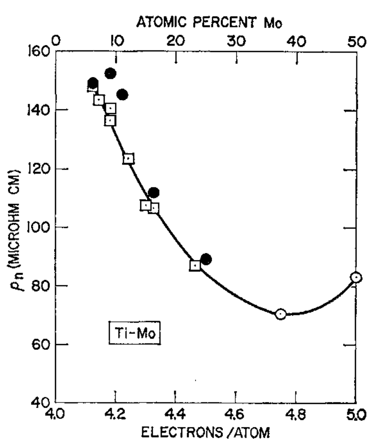

FIG. 6. Normal-state resistivity vs composition and electron concentration for Ti-Mo alloys. The circles represent data obtained at 1.2°K in this work for as-melted (unshaded points) and cold-rolled (shaded points) samples. The squares represent 4.2°K data (reference 45) for as-melted samples.

[37] P. R. Doidge, Phil. Trans. Roy. Soc. (London) **A248**, 553 (1956).
[38] B. B. Goodman, Phys. Rev. Letters **6**, 597 (1961).
[39] R. H. Parmenter, RCA Rev. **23**, 323 (1962).
[40] A. J. Glick and R. A. Ferrell, Bull. Am. Phys. Soc. **7**, 324 (1962).
[41] G. B. Yntema, in *Proceedings of the Eighth International Conference on Low Temperature Physics* [Butterworths Scientific Publications Ltd., London (to be published)].
[42] M. Tinkham, Phys. Rev. **129**, 2413 (1963).
[43] A. B. Pippard and V. Heine, Phil. Mag. **3**, 1046 (1958).
[44] A. M. Clogston, A. C. Gossard, V. Jaccarino, and Y. Yafet, Phys. Rev. Letters **9**, 262 (1962).

Actually the importance of such paramagnetic-energy considerations is not confined to the filamentary model, for, as already noted,[12] such factors were ignored in the GLAG theory. As a consequence, it is to be anticipated that the experimental upper critical field will in general be less than the smaller of H_{c2} and H_p. This is illustrated in Fig. 1 where the respective free energies $G_N(H)$ and $G_S(H)$ of the normal and superconducting states are plotted (schematically) vs magnetic field strength. If H_{c2} and H_p differ greatly in magnitude, as in the case illustrated, the experimental upper critical field should be only slightly less than the smaller of H_{c2} and H_p. However, if H_{c2} and H_p are comparable, the experimental upper critical field may be considerably less than the smaller of H_{c2} and H_p. On the other hand, a non-negligible normal-state diamagnetism and/or incomplete spin pairing in the superconducting state at $T=0$ could result in experimental upper critical fields larger than predicted by Eq. (14). It should, perhaps, be mentioned that the lower critical field should be relatively unaffected by normal-state paramagnetic considerations since H_{c1} values are always less than H_c (i.e., less than a few kG).

TABLE II. Values for ρ_n and $H_r(J=10,\ T=1.2)$ for Ti-Nb alloys.

At.% Nb	Reduction ratio	ρ_n ($\mu\Omega$ cm)	$H_r(J=10,\ T=1.2)$ (kG)	
10.0[a]	9.7	63.8	38.0	44.8
20.0[a]	14.3	97.2	98.0	108.0
25.0[a]	13.6	98.5	112.5	116.3
30.0	215.0	79.4	137.0	140.0
30.0	wire	85.7	136.2	...
34.1	wire	78.3	145.0	...
38.7	wire	63.0	145.0	...
42.5	193.0	58.7	144.0	146.0
43.7	wire	55.8	137.5	...
52.0	wire	49.3	125.0	...
60.0	269.0	42.2	123.0	129.0
70.0	15.6	30.6	104.4	112.0
85.0	17.3	19.0	58.0	64.0
90.0	45.3	12.0	51.3	58.7
95.0	56.4	6.8	33.2	39.9

[a] Mainly bcc but contained some second phase.

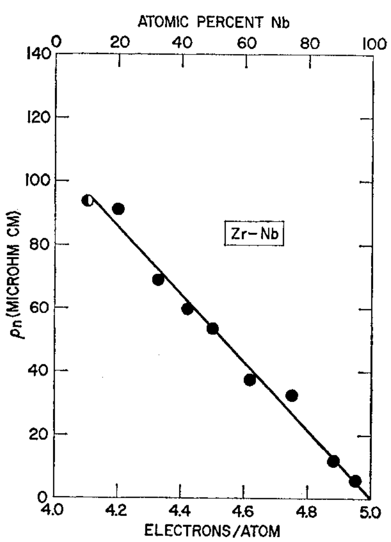

FIG. 7. Normal-state resistivity vs composition and electron concentration for Zr-Nb alloys at 1.2°K. The half-shaded point represents a sample comprised of more than one phase.

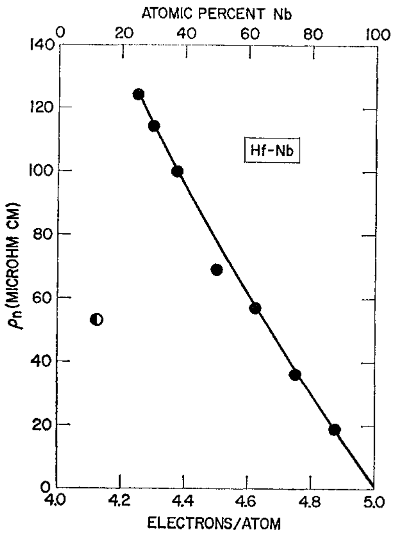

FIG. 8. Normal-state resistivity ρ_n vs composition and electron concentration for Hf-Nb alloys at 1.2°K. The half-shaded point represents a sample comprised of more than one phase.

III. EXPERIMENTAL SPECIMENS

Throughout this paper, alloy compositions are designated by the notation A-NB, where the two constituents are designated by A and B, and N refers to the atomic percentage of component B. The purity of starting materials was, in most cases, 99.9% or better. Most of the alloys studied were consolidated by melting the constituents together on the water-cooled copper hearth of a laboratory argon-arc furnace as previously described.[45] The alloy buttons (usually 1 to 2 cm in diameter) were all inverted and remelted at least six times in order to promote homogeneity. Rapid quenching of the melt, in direct contact with the copper hearth, occurred when the arc was broken. Because discussions of (and references on) the metallurgical character of the alloy systems studied have already been given in other works on the superconductivity of these alloy systems,[45–48] only scant mention of this aspect will be made herein. Nearly all the alloys studied were bcc, as determined from x-ray examinations of the small cold-rolled experimental specimens. The presence of phases other than bcc is indicated in the tables of experimental results which appear later and also (by half-shaded points) on the graphs showing the resistivity data. Because many of the alloys studied were metastable, the second phases were

[45] R. R. Hake, D. H. Leslie, and T. G. Berlincourt, J. Phys. Chem. Solids **20**, 177 (1961).

[46] J. K. Hulm and R. D. Blaugher, Phys. Rev. **123**, 1569 (1961).

[47] B. S. Chandrasekhar and J. K. Hulm, J. Phys. Chem. Solids **7**, 259 (1958).

[48] T. G. Berlincourt, J. Phys. Chem. Solids **11**, 12 (1959).

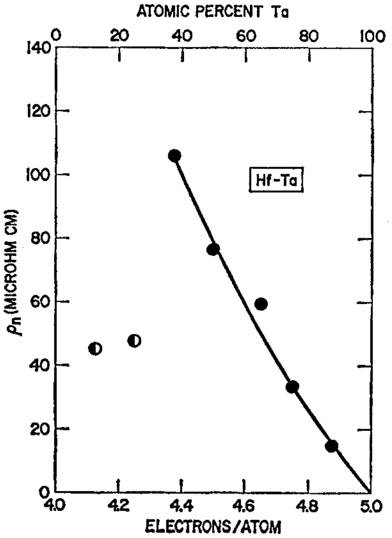

FIG. 9. Normal-state resistivity vs composition and electron concentration for Hf-Ta alloys at 1.2°K. The half-shaded points represent samples comprised of more than one phase.

often the product of cold-work-induced or low-temperature-induced martensitic transformations.

In most cases, the experimental specimens were ~1.3 cm long, ~0.02 to 0.08 cm wide, and ~0.005 cm thick. Usually, relatively thick sections (cut from the arc-melted buttons with a diamond cutoff wheel) were cold-rolled and sheared to produce the desired specimen geometry. The cold-rolling thickness reduction ratios for these samples are listed in the appropriate tables of experimental data. Some of the samples were obtained in the form of wire from Dr. J. Wong of the Wah Chang Corporation. Also, in a few instances, it was necessary to grind and polish the specimens to shape because of their brittle nature. However, all samples were copper-plated over a distance of ~0.3 cm on each end to facilitate soldering to the current leads.

TABLE III. Values of ρ_n and $H_r(J=10,\ T=1.2)$ for Ti-Ta alloys.

At.% Ta	Reduction ratio	ρ_n ($\mu\Omega$ cm)	$H_r(J=10,\ T=1.2)$ (kG)	
10.0[c]	21.6	35.7	42.2	47.0
19.8[b]	34.1	68.5	99.0	102.3
25.0[a]	8.7	78.8	108.0	112.0
29.5[a]	8.2	76.5	106.5	116.1
37.5	86.7	74.2	126.0	129.7
45.0	26.7	59.8	133.0	141.4
50.0	7.2	50.1	135.5	137.5
50.0	57.0	50.5	137.0	144.1
60.0	87.3	38.4	137.8	141.5
65.0	90.5	28.3	133.0	137.5
70.0	23.5	25.9	100.8	112.0
75.0	61.7	19.9	78.0	88.0
80.0	72.8	13.0	45.5	53.0
90.0	85.0	10.0	14.0	20.0

[a] Mainly bcc but contained some hcp.
[b] Bcc and hcp in roughly equal proportions.
[c] Mainly hcp but contained some bcc.

IV. APPARATUS AND METHOD

The measurements were carried out in pulsed magnetic fields up to ~160 kG. A standard four-probe resistivity measurement technique was used, and the sample could be mounted with its long axis either parallel or transverse to the magnetic field. For the latter case, the rolling (RP) plane could be oriented either parallel or transverse to the magnetic field. Potential probes separated by approximately 0.5 cm were securely clamped to the specimens, and great care was taken to avoid loops which could give rise to induced voltages during the magnetic-field pulse. Fortunately, an elaborate compensation scheme was not required, for it was found that induced voltages could be reduced to a nontroublesome level simply by an appropriate rotation of the sample probe about a vertical axis.[49] Spurious noise was reduced through the use of a high-cutoff filter.[49]

Data were recorded on a dual-beam oscilloscope as illustrated for a typical case in Fig. 2, where the magnetic field is shown rising sinusoidially from zero to 107 kG in 6.6 msec. Shortly after attainment of the maximum field the magnet was shorted, and the field decayed exponentially thereafter. The upper and lower wiggly traces represent, respectively, the voltage on the potential probes with and without a current density $J=10$ A/cm^2 flowing through the specimen for two successive magnetic-field pulses. The switching between superconducting and normal states is clearly discernible. The high reproducibility of the magnetic-field pulse is evident in that the traces for two successive pulses are indistinguishable.

TABLE IV. Values of ρ_n, H_r (J=10, T=1.2), and κ_l for Ti-Mo alloys.

At.% Mo	Reduction ratio	ρ_n ($\mu\Omega$ cm)	$H_r(J=10,\ T=1.2)$ (kG)		κ_l[a]
6.25	4.6	149.0	27.2	32.4	77.8
9.07	7.4	152.6	45.0	51.6	79.9
11.1	12.0	145.4	49.4	52.2	...
16.3	14.7	111.8	63.3	64.4	75.5
25.0	12.5	89.1	58.8	59.8	...
37.5	1.0	70.8	31.0	...	...
50.0	1.0	83.2	14.0	...	...

[a] For these alloys $\kappa_0 < 10^{-2}\kappa_l$ and, hence, $\kappa \approx \kappa_l$.

Several points should be mentioned with regard to the criteria used in the reduction of data of the type shown in Fig. 2. It might be argued that the field which restores half of the normal-state resistance should be chosen for comparison with the theory. However, if a certain width about H_{c2} is assumed for GLAG-type volume transition, and if it is further assumed that (1) the normal regions are uniformly nucleated and (2) they grow isotropically with increasing field, then it can

[49] We are indebted to Dr. A. C. Thorsen for suggesting these procedures.

be shown that the onset of resistance occurs only after a substantial amount of the material is normal. In contrast, full resistance is restored only after the entire volume of superconducting material has gone to zero. Whether or not this is actually the case might be answered in part by careful correlation of resistivity and specific-heat measurements. However, in view of this uncertainty and the sensitivity limitations of pulsed-field measurements, two fields are usually reported in this work, viz. (1) the field corresponding to the onset of a detectable resistance and (2) the field corresponding to the full restoration of resistance. In what follows, the symbol H$_r$ is used for simplicity to designate both of these fields, it being obvious that, when two values for H_r are given, the larger corresponds to the full restoration of resistance. In general, sufficient sensitivity was available so that for $J=10$ A/cm^2 a detectable departure of the resistivity from zero or ρ_n amounted to about 5 to 10% of ρ_n. Observed resistive transition widths usually increased with temperature but seldom exceeded

TABLE V. Values of ρ_n, $H_r(J=10,\ T=1.2)$, κ_0, and κ_l for Zr-Nb alloys.

At.% Nb	Reduction ratio	ρ_n ($\mu\Omega$ cm)	$H_r(J=10,\ T=1.2)$ (kG)		κ_0[b]	κ_l
10.2[a]	1.9	93.6	34.8	44.7	...	...
20.0	29.0	91.3	111.5	118.2	...	...
32.7	wire	68.8	126.3	129.7	...	...
40.0	...	...	...	...	4.5	54.2
42.1	19.1	59.8	119.5	124.0	...	...
50.0	9.4	53.6	113.0	120.8	...	...
62.0	6.7	37.3	109.9	114.8	...	...
75.0	12.5	32.6	102.4	110.1	...	...
88.2	8.2	12.0	63.0	78.0	...	...
90.0[c]	...	...	...	...	4.07 2.14	9.20 7.41
95.3	65.3	5.5	28.0	39.9	...	...
100.0[c]	...	...	...	...	2.5 1.3	...

[a] Mainly bcc but contained small amount of hcp.
[b] Calculated on the assumption that the Fermi surface area is given by 0.6 times the area of the free-electron sphere (see text).
[c] Two entries appear because of ambiguities in the value of γ (see text).

10% of H_r at 1.2°K, so that the lack of a precise criterion for the transition field was not too serious. Comparisons of steady-field and pulsed-field values for $H_r(J=10)$ revealed reassuring accord (~5%) for several Ti-Mo and Ti-V alloys which underwent transitions in fields less than 30 kG, although for some relatively dilute alloys long resistive tails were observed in steady fields which would surely be missed in less sensitive pulsed-field measurements.

In some of the pulsed-field measurements it was noted that even at low current densities the fields at which super-normal and normal-super transitions took place differed by as much as 5%. Such effects are to be expected at high current densities, where significant heating may occur in the normal state. However, the effects observed at low current densities did not correlate systematically with either ohmic heating or the rate of

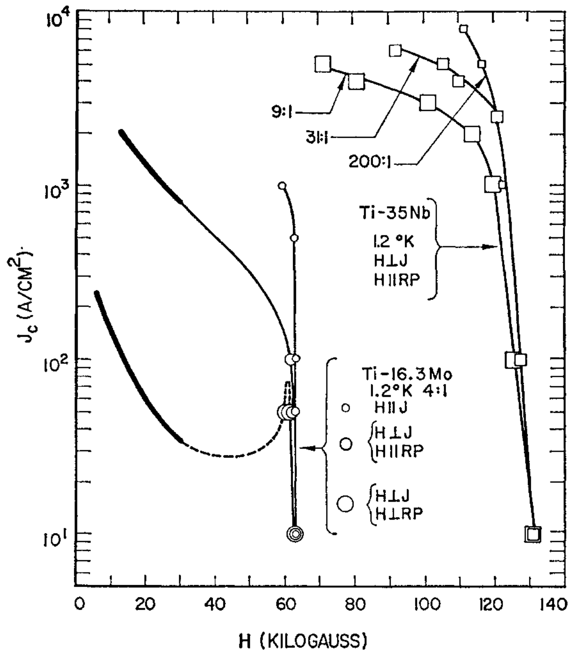

FIG. 10. Typical illustrations of the independence of $H_r(J\lesssim 10)$ upon cold working and relative orientations of H, J, and rolling-plane (RP) defect structure. The ratios indicate cold-rolling thickness reductions; heavy lines represent steady-field data; and the dashed line is an approximate representation based on observed resistive transitions.

change of magnetic field. Consequently, on the assumption that both of these effects would tend to depress the transition field, the higher of the two transition fields [H_r(supernormal) and H_r(normal-super)] was assumed to be the more nearly correct.

Knowledge of the normal-state electrical resistivity is essential to a comparison of experiment with the GLAG theory [Eqs. (12) and (13)]. In general, resistivity values were deduced at 1.2°K for a measuring current density of 1000 A/cm^2, so that the accuracy in this determination was considerably greater than could be achieved from a low-measuring-current recording of the type shown in Fig. 2. Estimated errors arising from uncertainties in sample dimensions and oscilloscope cali-

TABLE VI. Values of ρ_n and $H_r(J=10,\ T=1.2)$ for Hf-Nb alloys.

At.% Nb	Reduction ratio	ρ_n ($\mu\Omega$ cm)	$H_r(J=10,\ T=1.2)$ (kG)	
12.5[a]	8.6	53.2	83.0	96.0
25.0	17.3	124.4	83.1	89.7
30.0	8.6	114.4	95.1	98.8
37.5	16.7	100.3	99.5	103.5
50.0	98.7	69.0	102.4	109.4
62.5	14.1	57.2	91.0	101.6
75.0	7.7	36.3	78.9	89.6
87.5	15.1	19.1	62.1	69.6

[a] Bcc and hcp in roughly equal proportions.

TABLE VII. Values of ρ_n and $H_r(J=10,\ T=1.2)$ for Hf-Ta alloys.

At.% Ta	Reduction ratio	ρ_n ($\mu\Omega$ cm)	$H_r(J=10,\ T=1.2)$ (kG)	
12.5[a]	7.1	45.5	57.6	82.5
25.0[a]	1.0	48.1	42.1	57.1
37.5	2.2	106.0	80.5	87.5
50.0	3.1	76.7	84.5	90.0
65.0	6.2	59.5	84.2	93.2
75.0	4.2	33.3	65.0	72.3
87.5	6.3	15.0	36.6	56.3

[a] Mainly hcp but contained some bcc.

bration led to a probable error of $\pm 10\%$, but, as is evident below, the consistency of the data suggests that this estimate might be overly pessimistic.

V. EXPERIMENTAL RESULTS

A. Normal-State Resistivities

Extensive normal-state resistivity data are presented in Figs. 3–9 and Tables I–VIII for the nine alloy systems studied in this investigation. The composition dependences of ρ_n for the Group IV–Group V alloys are all qualitatively similar in that ρ_n falls approximately linearly from a high value (80 to 140 $\mu\Omega$ cm) at the phase stability limit on the Group IV-rich side of the phase diagram to approximately zero for the pure Group V element. This unusual behavior, which has been noted and discussed for several of these alloy systems,[45] permits a very qualitative judgement to be made of the reliability of the superconductivity determinations for the two-phase samples (half-shaded points). Simply stated, the greater the deviation of a half-shaded (or two-phase) point from the linear extrapolation of the ρ_n vs composition curve, the less meaningful the corresponding resistive critical field value is likely to be.

The normal-state resistivity data for the Ti-Mo system are worthy of further comment. In Fig. 6, the unshaded squares (data from reference 45) and circles correspond to samples which were ground and polished to shape, whereas the shaded points correspond to cold-worked samples. Although the cold-worked sample points fall systematically higher, the difference does not exceed the probable error of the present determinations. As has previously been noted,[16] this result suggests that in such concentrated alloys atomic disorder is much more important than the dislocation content in determining ρ_n. The minimum in Fig. 6 is a surprising feature which should be checked by more precise experimental techniques.

B. Upper-Critical-Field Criterion

In the attempt to compare experiment with the "homogeneous" theory it was first necessary to ascertain whether an experimental upper-critical-field criterion could be established which could indeed be attributed to the bulk character rather than the defect character of the experimental specimen. Except for ρ_n, the parameters which determine H_{c2} in the GLAG theory and H_p in Clogston's criterion are, in general, almost independent of dislocation content. As discussed in the previous section, even ρ_n is little affected by dislocation content in concentrated solid-solution alloys. Consequently, for alloys of the type considered in this

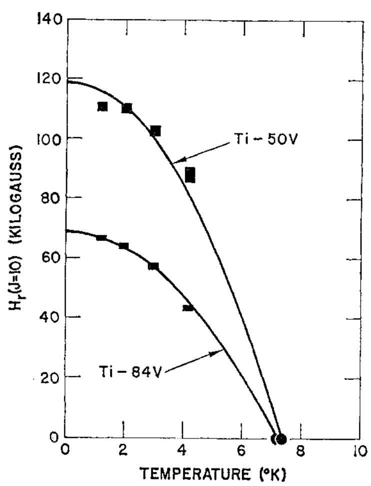

FIG. 11. $H_r(J=10)$ vs T for Ti-50 V and Ti-84 V. The vertical extent of each rectangular point represents the range in magnetic field between the onset of a detectable resistance and full restoration of the normal-state resistance. The circles represent the T_c data of Cheng *et al.* (reference 62). Parabolas have been fitted roughly to the data to show the nature of typical deviations.

work, the theoretically predicted upper critical field should be nearly independent of (1) the amount and type of cold working and (2) the relative orientations of H and any existing anisotropic extended-defect structures. (This assumes, of course, that cold working does not induce martensitic phase transformations.) Within the sensitivity limitations already discussed, such behavior was indeed found to be characteristic of experi-

TABLE VIII. Values of ρ_n, $H_r(J=10,\ T=1.2)$, $H_p(T=1.2)$, $H_{c2}(T=1.2)$, and κ_l for U-Nb and U-Mo alloys.

Alloy	Reduction ratio	ρ_n ($\mu\Omega$ cm)	$H_r(J=10,\ T=1.2)$ (kG)		$H_p(T=1.2)$ (kG)	$H_{c2}(T=1.2)$ (kG)	κ_l[a]
U-22.2 Nb	3.3	75.7	23.2	26.9	23.0	35.0	64.8
U-11.6 Mo	1.0	80.9	21.0	29.0	19.8	36.2	73.8
U-21.7 Mo	3.5	74.0	29.1	32.0	25.1	36.3	62.2
U-30.5 Mo	2.2	79.2	26.0	30.0	22.8	33.8	65.3

[a] For these alloys $\kappa_0 < 10^{-2}\kappa_l$ and, hence, $\kappa \approx \kappa_l$.

[50] T. G. Berlincourt, Phys. Rev. 114, 969 (1959).

mentally determined resistive critical fields measured at low enough current densities. This was pointed out in our earlier work[12,24–26] and is again illustrated for emphasis in Fig. 10. In this figure, the current density corresponding to the onset of a detectable resistance is plotted against magnetic field for a wide range of cold-rolling reduction ratios and a variety of relative orientations of H, J, and specimen rolling plane (RP). Similar results were also obtained for concentrated alloys in the Ti-V and Ti-Ta systems. For pure metals and dilute alloys, in which cold working markedly affects ρ_n, quite different results are, of course, to be expected and are, in fact, observed.[50] Subject to this restriction, at current densities $J \lesssim 10\mathrm{A/cm}^2$ the field which first restores a detectable resistance appears to be characteristic of the bulk material (rather than dislocation structure or experimental geometry) and, hence, should

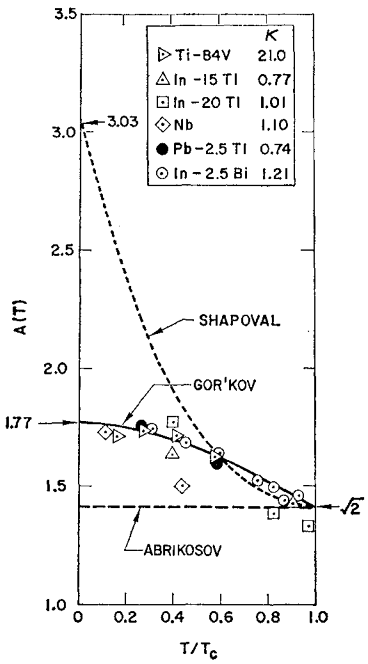

FIG. 12. Values of $A(T) = H_{c2}/\kappa H_c$ predicted according to Abrikosov [Eq. (4)], Gor'kov [Eq. (5)], and Shapoval [Eq. (6)] compared with data on a number of superconductors of the second kind. Ti-84 V, this work; In-15 Tl and In-20 Tl, Stout and Guttman (references 54 and 55); Nb, Stromberg and Swenson (reference 58); Pb-2.5 Shubnikov *et al.* (reference 59); In-2.5 Bi, Kinsel *et al.* (reference 60).

be approximately identifiable with H_{c2} or H_p. The field $H_r(J=10)$ was chosen for comparison in this work because it appeared to represent the best compromise between the available detection sensitivity and the allowable perturbation of the high-field superconducting state by measuring current. It may be noted in Fig. 10 that H_r remains slightly current-density dependent in the vicinity of $J=10$ A/cm². In order to establish that dH_r/dJ was indeed small in the vicinity of $J=10$ A/cm², H_r was generally determined at 10, 30, 100, and 1000 A/cm². It may also be remarked that most of the measurements reported in this work were made with $H \perp J$ and $H \| RP$ (although, as discussed above, the results were relatively insensitive to this consideration).

The marked influence of defect structure and experimental geometry on H_r at high transport-current den-

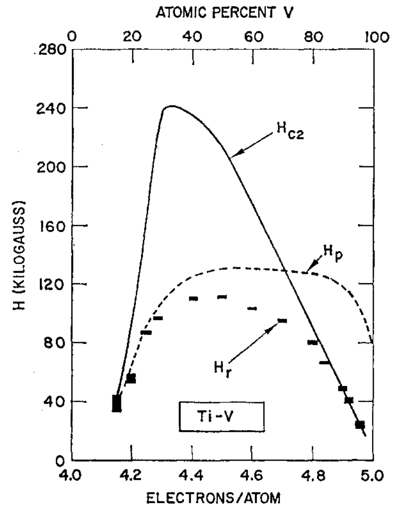

FIG. 13. $H_r(J=10,\ T=1.2)$, $H_{c2}(T=1.2)$, and $H_p(T=1.2)$ vs composition and electron composition for Ti-V alloys. The vertical extent of each rectangular point represents the range in magnetic field between the onset of a detectable resistance and full restoration of the normal-state resistance. Excellent quantitative accord is obtained between $H_r(J=10,\ T=1.2)$ and $H_{c2}(T=1.2)$ for V-rich alloys. Elsewhere limits appear to be imposed by Clogston's criterion as shown by the near agreement between $H_r(J=10,\ T=1.2)$ and $H_p(T=1.2)$.

sities is also shown in Fig. 10, where the typical defect-induced[15–18,51] enhancement, anisotropy, and "peak effect" in J_c are illustrated. In this connection, it is noteworthy that pulsed-magnetic-field measurements enjoy one advantage over steady-field measurements in permitting a study of the form of the resistive transition in cases where the large current densities would lead to prohibitive ohmic heating in steady fields.

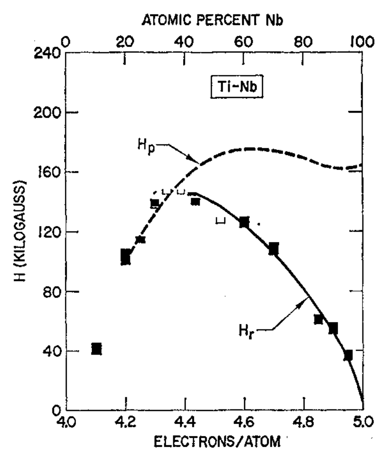

FIG. 14. $H_r(J=10,\ T=1.2)$ and $H_p(T=1.2)$ vs composition and electron concentration for Ti-Nb alloys. The vertical extent of each rectangular point represents the range in magnetic field between the onset of a detectable resistance and full restoration of the normal-state resistance. Only the onset was observed for the U-shaped points.

[51] R. R. Hake, T. G. Berlincourt, and D. H. Leslie, Bull. Am. Phys. Soc. 7, 474 (1962).

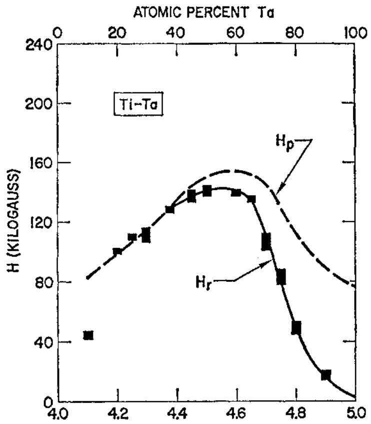

FIG. 15. $H_r(J=10, T=1.2)$ and $H_p(T=1.2)$ vs composition and electron concentration for Ti-Ta alloys. The vertical extent of each rectangular point represents the range in magnetic field between the onset of a detectable resistance and full restoration of the normal-state resistance.

C. Temperature Dependence of $H_r(J=10)$

Various forms for the temperature dependence of H_{c2} are predicted in Eqs. (4)–(6). As a test of this aspect of the GLAG theory, we determined $H_r(J=10)$ at temperatures of approximately 1.2, 2.0, 3.0, and 4.2°K for 13 different alloy compositions. In every instance, a nearly parabolic dependence was observed as in the case of the thermodynamic critical field. (The T_c data of Hulm and Blaugher[46] were used for the end point in most of these curves.) Although departures from T^2 behavior (both higher and lower powers of T) were usually observed, all such curves appeared to approach 0°K with approximately zero slope. This is illustrated for Ti-50 V and Ti-84 V in Fig. 11, where parabolas have been fitted roughly to the data to show the nature of typical deviations. Evidence to be presented below suggests that the transition in Ti-84 V is almost purely GLAG type while that in Ti-50 V may be paramagnetically limited. Differences in the form of the temperature dependence might, therefore, be anticipated for these two alloys. Unfortunately, the limited accuracy of the present measurements argues against attaching much significance to differences evident in Fig. 11. This point should, however, be pursued via the more precise steady-field measurement techniques. In any event, the data obtained in this study plus other results[52] on $H_r(T)$ appear to be in direct contradiction with Shapoval's predictions, Eq. (6), of a nearly linear $H_{c2}(T)$ curve with large slope at $T=0$.

The considerable variation in the form of $H_r(T)$ observed for different alloys in this study (as well as in the studies of Wernick *et al.*[52]) suggests that deviations from a law of corresponding states may well exist and significantly exceed the well-known variations in $H_c(T)$.[53] Nevertheless, an attempt was made to ascertain the approximate form for the temperature dependence of the upper critical field for cases in which normal-state paramagnetic free-energy considerations are unimportant. In Fig. 12, values of $A(T)=H_{c2}/\kappa H_c$ predicted by Abrikosov [Eq. (4)], Gor'kov [Eq. (5)], and Shapoval [Eq. (6)] are compared with data on a number of superconductors of the second kind. The values of $A(T)$ plotted for Ti-84 V were deduced using the half-resistance $H_r(J=10)$ data of Fig. 11, a value of $\kappa=21.0$ (calculated as explained in the next section), and values for H_c calculated from Eq. (1). The accord with Gor'kov's prediction is remarkable, although it could be fortuitous. The remaining $A(T)$ data in Fig. 12 correspond to values of $H_{c2}(T)$ deduced from the *magnetic-moment measurements* of a number of investigators on a variety of superconductors of the second kind. That some of the single-crystal In-Tl alloys studied several years ago by Stout and Guttman[54,55] were superconductors of the second kind has already been suggested,[56] and the corresponding $A(T)$ values are plotted in Fig. 12 for In-15 Tl (with $\kappa=0.77$) and In-20 Tl (with $\kappa=1.01$). These κ values were estimated[57] from the ρ_n, H_0, and T_c data of Stout and Guttman and Eqs. (1) and (12). The diamond-shaped points correspond to the Nb data of Stromberg and Swenson[58] who estimated $\kappa=1.1$. The

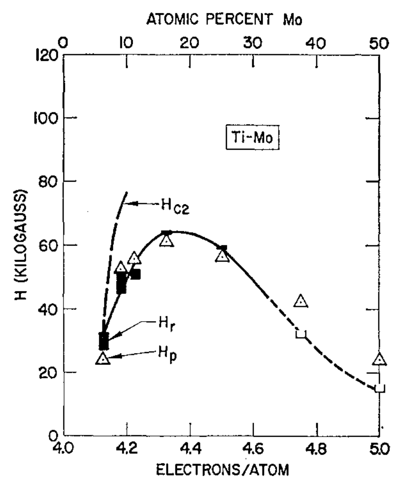

FIG. 16. $H_r(J=10, T=1.2)$, $H_{c2}(T=1.2)$, and $H_p(T=1.2)$ vs composition and electron concentration for Ti-Mo alloys. The vertical extent of each rectangular point represents the range in magnetic field between the onset of a detectable resistance and the full restoration of the normal-state resistance. Only the onset was observed for the U-shaped points.

[52] J. H. Wernick, F. J. Morin, F. S. L. Hsu, D. Dorsi, J. P. Maita, and J. E. Kunzler, *High Magnetic Fields* (Tech Press, Cambridge, Massachusetts and John Wiley & Sons, Inc., New York, 1962), p. 609.

[53] D. E. Mapother, IBM J. Res. Develop. **6**, 77 (1962).

[54] J. W. Stout and L. Guttman, Phys. Rev. **88**, 703 (1952).

[55] J. W. Stout and L. Guttman, Phys. Rev. **88**, 713 (1952).

[56] T. G. Berlincourt, remarks at Eighth International Conference on Low-Temperature Physics, London, 1962 (unpublished).

[57] A value of $H_0=280$ G was assumed for In-20 Tl, inasmuch as Stout and Guttman (references 54 and 55) incorrectly identified the lower critical field with the thermodynamic critical field.

[58] T. F. Stromberg and C. A. Swenson, Phys. Rev. Letters **9**, 370 (1962).

shaded circles correspond to the Pb-2.5 Tl data of Shubnikov *et al.*[59] with κ chosen to give a reasonable fit to the Gor'kov curve. The open circles represent the data of Kinsel *et al.*[60] for In-2.5 Bi with $\kappa = 1.21$, which is about 4% less than the average of their four independent determinations. The latter data, which are the most complete and probably the most reliable in Fig. 12, are in excellent accord with Gor'kov's prediction.[61] On the other hand, the Nb data might be interpreted as an intermediate case, and, by an adjustment of κ, the In-20 Tl data could be shifted to approach Shapoval's $A(T)$. However, the preponderance of existing data on $A(T)$ is reasonably consistent with Gor'kov's predictions and clearly at variance with the predictions of Abrikosov and Shapoval.

With regard to the lower critical field, it is worth mentioning at this point that Stromberg and Swenson[58] and Kinsel *et al.*[60] found H_{c1}/H_c to be temperature-independent to within a few percent, in keeping with the prediction of Eq. (3).

D. Composition Dependence of $H_r(J=10,\ T=1.2)$ and Comparison with $H_{c2}(T=1.2)$ and $H_p(T=1.2)$

In Figs. 13–19 and Tables I–VIII, experimental values of $H_r(J=10,\ T=1.2)$ are presented for alloys in the systems Ti-V, Ti-Nb, Ti-Ta, Ti-Mo, Zr-Nb, Hf-Nb,

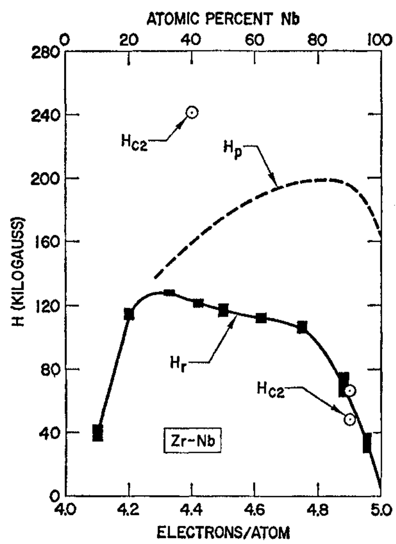

FIG. 17. $H_r(J=10,\ T=1.2)$, $H_{c2}(T=1.2)$, and $H_p(T=1.2)$ vs composition and electron concentration for Zr-Nb alloys. The vertical extent of each rectangular point represents the range in magnetic field between the onset of detectable resistance and the full restoration of the normal-state resistance. Two values of $H_{c2}(J=10,\ T=1.2)$ are shown for Zr-90 Nb because of ambiguities in the experimental determination of γ (see text).

[59] L. W. Shubnikov, W. I. Kotkevich, J. D. Shepelev, and J. N. Riabinin, Zh. Eksperim. i Teor. Fiz. **7**, 221 (1937).

[60] T. Kinsel, E. A. Lynton, and B. Serin, Phys. Letters **3**, 30 (1962).

[61] Kinsel *et al.* (reference 60) incorrectly interpret their data as favoring Shapoval's predicted temperature dependence of H_{c2}.

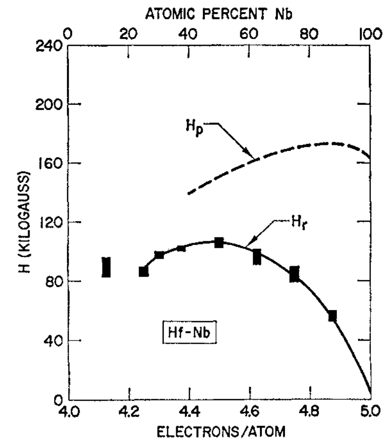

FIG. 18. $H_r(J=10,\ T=1.2)$ and $H_p(T=1.2)$ vs composition and electron concentration for Hf-Nb alloys. The vertical extent of each rectangular point represents the range in magnetic field between the onset of detectable resistance and the full restoration of the normal-state resistance.

Hf-Ta, U-Nb, and U-Mo. The vertical extent of each rectangular point in the figures corresponds to the range of magnetic field over which the resistance increased from a detectable level to the full normal-state resistance. The U-shaped points correspond to samples for which only the onset of resistance was determined.

For all the Group IV–Group V alloys, $H_r(J=10,\ T=1.2)$ peaks up sharply between 4 and 5 "valence" electrons per atom (e/a). The behavior is in accord with Eq. (13) and the well-known peaking of ρ_n, γ, and T_c between the same electron concentrations. It is noteworthy that ρ_n, which rises from 0 at both 4 and 5 e/a to $\sim 100\ \mu\Omega$ cm in between, is a much stronger function of alloy composition than either γ or T_c and, therefore, may be considered to be more responsible for the marked peaking in $H_r(J=10,\ T=1.2)$. Although the lack of data on γ precluded a quantitative comparison between $H_r(J=10,\ T=1.2)$ and $H_{c2}(T=1.2)$ for the systems Ti-Nb, Ti-Ta, Hf-Nb, and Hf-Ta, ρ_n data have been presented above in anticipation that such data may become available.

Ti-V Data

The most extensive comparison between $H_r(J=10,\ T=1.2)$ and $H_{c2}(T=1.2)$ was possible for Ti-V alloys, for which the most complete low-temperature electronic specific heat data exist. This is a fortunate circumstance, for, as indicated in Table I and Fig. 13, this same alloy system was characterized by very narrow resistive-transition breadths. Values for κ_l were deduced from Eq. (12) using smoothed curve values of ρ_n (Fig. 3) and γ from the work of Cheng *et al.*[62] Approximate values for κ_0 were estimated using Eq. (11) and the γ and T_c data of the same investigators. As in earlier work,[38] it

[62] C. H. Cheng, K. P. Gupta, E. C. van Reuth, and P. A. Beck, Phys. Rev. **126**, 2030 (1962).

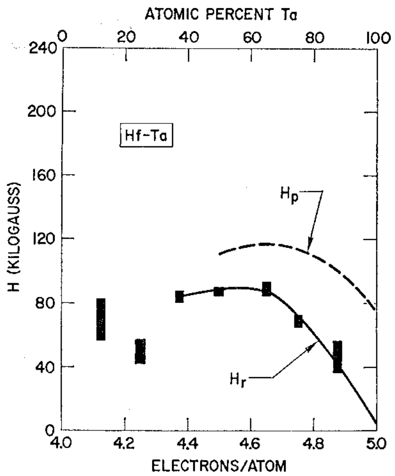

FIG. 19. $H_r(J=10,\ T=1.2)$ and $H_p(T=1.2)$ vs composition and electron concentration for Hf-Ta alloys. The vertical extent of each rectangular point represents the range in magnetic field between the onset of a detectable resistance and the full restoration of the normal-state resistance.

was assumed that $S/S_f=0.6$ where S_f is the area of the Fermi surface for a free electron gas of the same density as in the alloy under consideration. This is admittedly a very uncertain estimate, but the error in κ resulting from a poor estimate of S/S_f is relatively small because $\kappa_l \gg \kappa_0$ for all the alloys described herein. Values of κ, κ_0, and κ_l so deduced are listed in Table IX, and κ is plotted against electron concentration in Fig. 20. These values of κ and values of H_c obtained through the use of Eq. (1) permitted calculations of $H_{c2}(T=1.2)$ according to the predictions of Eq. (5). [Empirical justification for the choice of Eq. (5) was presented in the preceding section.] In Fig. 13, the $H_{c2}(T=1.2)$ values so obtained are compared with $H_r(J=10,\ T=1.2)$. For V-rich alloy compositions, T_c is relatively large and ρ_n is small, so that comparisons with the GLAG theory should be relatively unperturbed by the normal-state paramagnetic energy considerations which lead to the Clogston criterion. In accord with this prediction, excellent quantitative agreement is evident in Fig. 13 for V-rich alloy compositions. For other compositions, $H_{c2}(T=1.2)$ is significantly greater than $H_r(J=10,\ T=1.2)$, and limitations are apparently imposed by Clogston's criterion. Indeed, values for $H_p(T=1.2)$, calculated using Eq. (14), agree remarkably well with $H_r(J=10,\ T=1.2)$ over a considerable range of composition. As mentioned earlier, the observed low-current-density resistive critical field should be less than the smaller of the two fields H_{c2} and H_p. Considered in this light, the fit between experiment and theory must be considered as quite satisfactory for Ti-V alloys.

A test of this viewpoint is possible. If the GLAG theory is correct, except for its neglect of the normal-state paramagnetic energy, and if the discrepancy between H_r and H_{c2} for an alloy such as Ti-40 V is due *only* to this neglect, then the experimental lower critical field for this alloy should be in agreement with H_{c1} calculated using either Eq. (3) or Goodman's interpolated curve,[22] whichever is applicable. This follows because the normal-state paramagnetic energy is negligible for fields of the order of H_{c1} (which is always less than H_c). Predicted values of $H_{c1}(T=1.2)$ are presented in Fig. 20. Experimental determinations for comparison with these values would be of great interest as a direct test of the GLAG theory and an indirect test of the Clogston criterion.

Ti-Nb Data

In Fig. 14, $H_r(J=10,\ T=1.2)$ data for Ti-Nb alloys are compared with $H_p(T=1.2)$ calculated on the basis of the T_c data of Hulm and Blaugher.[46] A range of excellent agreement is evident for compositions between approximately 20 and 40 at.% Nb, but agreement is quite poor for Nb-rich alloys, where the upper critical field is most likely given approximately by the GLAG theory. It may be noted that more careful control of specimen quality has removed some of the scatter evident in our preliminary Ti-Nb results.[12] The peak resistive critical field of 145 kG occurring in the vicinity of Ti-40 Nb is, as far as we know, the highest yet reported for a ductile alloy. We have already reported critical current density data[24–26] which suggest that this system possesses considerable potential for superconducting-magnet application.

Ti-Ta Data

In Fig. 15 the low-current-density resistive critical fields for Ti-Ta alloys are compared with $H_p(T=1.2)$. The latter curve was calculated using T_c data recently obtained by Blaugher and Joiner[63] on the same alloy buttons used in this study. Excellent agreement between

TABLE IX. Values of κ_0, κ_l, κ, and $H_{c1}(T=1.2)$ for Ti-V alloys.

at.% V	κ_0[a]	κ_l	κ	$H_{c1}(T=1.2)$ (G)
15.0	0.26	86.5	86.8	13
20.0	0.58	90.8	91.4	23
25.0	1.16	94.0	95.2	38
30.0	1.81	92.5	94.3	52
40.0	2.02	77.2	79.2	69
50.0	2.12	63.7	65.8	87
60.0	2.13	49.7	51.8	109
70.0	2.08	36.6	38.7	140
75.0	2.02	30.9	32.9	156
80.0	1.93	25.2	27.1	179
85.0	1.80	19.5	21.3	205
90.0	1.60	14.3	15.9	238
95.0	1.35	8.0	9.4	311
100.0	0.90[b]	0.0	0.9	922

[a] Calculated on the assumption that the Fermi surface area is given by 0.6 times the area of the free electron sphere (see text).
[b] Preliminary experimental data (reference 58) suggest a value $\kappa_0 \lesssim 1.4$ for pure V.

[63] R. D. Blaugher and W. C. H. Joiner (private communication).

$H_r(J=10,\ T=1.2)$ and $H_p(T=1.2)$ extends over a particularly broad range of composition for this system, but again agreement is very poor for Group V-rich alloys, where H_{c2} is most likely less than H_p.

Ti-Mo Data

In Fig. 16, $H_{c2}(T=1.2)$ and $H_p(T=1.2)$ are compared with the low-current-density resistive critical fields of Ti-Mo alloys. The low-temperature specific heat data of Hake[64] were used in calculating κ_l and $H_{c2}(T=1.2)$, and the T_c data of Blaugher *et al.*[65] were used in deducing $H_p(T=1.2)$. Again the experimental upper critical fields are in good accord with H_p between approximately 4.1 and 4.6 e/a. The dotted portion of the experimental curve determined by the 37.5 and 50 at.% Mo alloys is somewhat uncertain. These alloys were too brittle to be cold rolled and were, therefore, measured at current densities down to 1 A/cm^2 in steady magnetic fields. Even so, the J_c vs H_r curves were not steep enough to define the resistive critical field with much certainty.

Zr-Nb Data

The experimental and theoretical upper critical fields for Zr-Nb alloys are presented in Fig. 17. The low-temperature specific heat data of Morin and Maita[66] and the T_c data of Hulm and Blaugher[46] were used in calculating values for κ_0, κ_l, $H_{c2}(T=1.2)$ and $H_p(T=1.2)$. The results follow the general pattern evident in alloy systems already discussed, i.e., the upper critical fields of the Group V-rich alloys appear to be determined principally by the GLAG theory, and the Clogston criterion apparently imposes a limit for Group IV-rich alloys. The double entries in Table V for Zr-90 Nb and pure Nb and the two $H_{c2}(T=1.2)$ values for Zr-90 Nb in Fig. 17 correspond to the two γ values given for each of these samples by Morin and Maita.[66] They observed anomalies in the low-temperature specific heat which led to ambiguities in the determination of γ. However, thermodynamic consistency appears to exist between the H_c value deduced from the magnetization data of Stromberg and Swenson[58] and the lower γ value for pure Nb, suggesting that the lower of the two values given for κ_0, κ_l, and $H_{c2}(T=1.2)$ is in each case the correct one. It is of interest that if $S/S_f=0.6$ (as has been assumed throughout this work), then $\kappa_0=1.3$ for pure Nb in good accord with the experimental value $\kappa=1.1$ given by Stromberg and Swenson. The result $S/S_f=0.18$ obtained by these authors is erroneous.

Hf-Nb and Hf-Ta Data

In Figs. 18 and 19, the experimental upper critical fields for Hf-Nb and Hf-Ta alloys are compared with values of H_p calculated using the T_c data of Hulm and Blaugher.[46] The discrepancies for the Hf-Nb alloys are large enough to suggest that the experimental upper critical fields might be determined principally by the GLAG theory over a considerable range of composition. For this reason, measurements of γ for Hf-Nb alloys would be of particular interest.

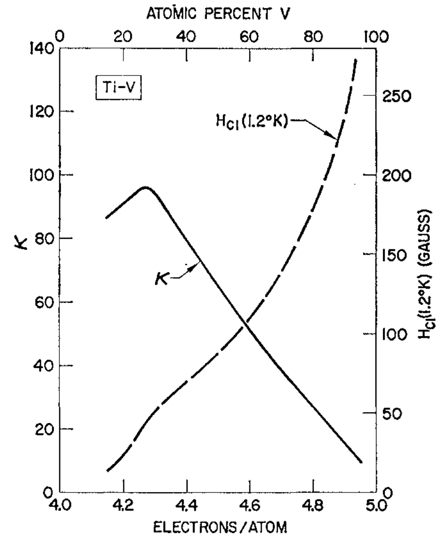

FIG. 20. κ and approximate theoretical values for $H_{c1}(T=1.2)$ vs composition and electron concentration for Ti-V alloys.

U-Nb and U-Mo Data

The experimental upper-critical-field data for U-Nb and U-Mo alloys are compared with $H_{c2}(T=1.2)$ and $H_p(T=1.2)$ in Table VII. The low-temperature specific heat data of Goodman[67] (extrapolated in several instances) and the transition-temperature data of Berlincourt[48] were used in the calculations of κ_l, $H_{c2}(T=1.2)$ and $H_p(T=1.2)$. The agreement between experiment and theory can be considered as reasonable in view of the considerable uncertainties in the experimental quantities used in these comparisons.

VI. DISCUSSION

A. Summary of Present Results

The experimental results of this investigation may be briefly summarized as follows:

(1) The low-current-density resistive critical fields for a number of *concentrated* transition metal alloys are nearly independent of the amount of cold working and the relative orientations of magnetic field, current, and defect structure. This is consistent with the view that

[64] R. R. Hake, Phys. Rev. **123**, 1986 (1961).

[65] R. D. Blaugher, B. S. Chandrasekhar, J. K. Hulm, E. Corenzwit, and B. T. Matthias, J. Phys. Chem. Solids **21**, 252 (1961).

[66] F. J. Morin and J. P. Maita, Phys. Rev. **129**, 1115 (1963).

[67] B. B. Goodman, J. Hillairet, J. J. Veyssie, and L. Weil, Compt. Rend. **250**, 542 (1960); also in *Proceedings of the Seventh International Conference on Low-Temperature Physics*, edited by G. M. Graham and A. L. Hallis Hallet (University of Toronto Press, Toronto, 1961), p. 350.

the low-current-density resistive critical field is a function of bulk electronic parameters quite independent of extended defect considerations.

(2) The low-current-density resistive critical fields of Group IV–Group V transition metal alloys peak up sharply in the vicinity of 4.5 e/a, an electron concentration at which peaking also typically occurs for such (approximately) defect-independent alloy parameters as T_c, H_c, and γ.

(3) The low-current-density resistive critical field may be identified approximately with H_{c2} (the upper critical field of the GLAG theory) or H_p(Clogston's limiting field) whichever is smaller. Indeed, in comparisons of measured low-current-density resistive critical fields with H_{c2} and H_p, *excellent quantitative accord has been achieved without adjustable parameters.* A pattern exists for Group IV–Group V transition metal alloys in that the experimental upper critical fields for Group V-rich compositions appear to be determined principally by the GLAG theory, while for other compositions limitations appear to be imposed by normal-state paramagnetic free-energy considerations. This is readily understood in terms of the low normal-state resistivities and high transition temperatures of Group V-rich alloys. The accord with H_p is in many instances better than anticipated in view of the fact that H_p is merely an upper limit (see Fig. 1). Good agreement in cases (such as Ti-rich Ti-V alloys) where H_{c2} and H_p are nearly equal might be interpreted as evidence that the normal-state diamagnetism is appreciable and/or spin pairing is incomplete in the superconducting state.

(4) The existing experimental data on the form of the temperature dependence of H_{c2} favor the predictions of Gor'kov over those of Abrikosov and of Shapoval. However, a need exists for additional data bearing on this point.

B. Other Evidence in Accord with the GLAG Theory

Recent measurements by a number of investigators have provided additional evidence in support of the GLAG theory.

(1) Low-temperature specific heat measurements on V_3Ga have been carried out by Morin *et al.*[68] in magnetic fields up to 70 kG. These studies revealed that the high-field superconducting transition (i) occurs without latent heat after nearly complete flux penetration and (ii) involves the main bulk of the electronic assembly. Both of these points (originally interpreted as evidence for a large number of "filaments") are in full accord with the predictions of the GLAG theory. Moreover, these calorimetrically determined bulk high-field transitions occurred at fields nearly coincident with low-current-density resistively determined upper critical fields,[52] thus providing further justification for the approximate identification of the latter with H_{c2} in the present work.[68a]

(2) In studies of the magnetization curves of a number of homogeneous, strain-free, low-melting-point alloys, Bon Mardion *et al.*,[69] Livingston,[70] and Kinsel *et al.*[60] have observed a very close approach to reversibility. Furthermore, the alloys studied were in general characterized by upper critical fields of the order of a few kilogauss so that normal-state paramagnetic free-energy contributions were negligible, and exact comparisons could be made with a number of features of the Abrikosov-type magnetization curve. In fact, for In-2.5 Bi near T_c [where Eqs. (4)–(6) all yield $A(T)=\sqrt{2}$], Kinsel *et al.*[60] were able to show that a value of κ deduced from the experimental quantities κ_0, ρ_n, γ, and T_c could be used to predict values for H_{c1}, H_{c2}, and $(dM/dH)_{H_{c2}}$ in excellent accord with observation.

(3) Gor'kov[11] has emphasized that superconducting behavior of the second kind is not necessarily confined to alloys, inasmuch as defect-free elemental superconductors for which $\kappa_l\approx 0$ may nevertheless be characterized by $\kappa_0>1/\sqrt{2}$. That such should also be the case for a perfect crystal of an intermetallic compound such as V_3Ga has been pointed out by Goodman.[71] Furthermore, the data of Stromberg and Swenson discussed above were obtained with very high purity Nb, for which it is probably true that $\kappa_0\approx\kappa\approx 1.1$. The studies of Autler *et al.*[72] on impure Nb also support this view, for these investigators observed that κ vs ρ_n extrapolates to a value of $\kappa_0\approx 1.3$ at $\rho_n=0$.

(4) Swartz[73] has recently carreid out magnetization measurements on (presumably inhomogeneous) samples of Nb_3Sn, Nb_3Al, V_3Ga, and V_3Si characterized by large κ and irreversible size-dependent magnetization curves. In the limit of small specimen size the departure of the magnetization curves from linearity occurred for fields considerably less than H_c and roughly in accord with expectation for H_{c1}. Similar results have been obtained by Hauser[74] for thin samples of V_3Si and by

[68] F. J. Morin, J. P. Maita, H. J. Williams, R. C. Sherwood, J. H. Wernick, and J. E. Kunzler, Phys. Rev. Letters **8**, 275 (1962).

[68a] *Note added in proof.* Recent specific-heat measurements by R. R. Hake on a *well-annealed* superconducting alloy V-5 Ta [$T_c=4.3$°K, $\rho_n=7.7\times10^{-6}$ Ω-cm, $\gamma=1.0\times10^4$ erg/cm^3 (K°)^2, $\kappa\approx 7$] reveal relatively sharp ($\Delta T\approx 0.1$/°K), bulk specimen, reversible, second-order superconducting transitions at temperatures T_s somewhat below T_c in magnetic fields ($H\leq 4$ kG) much larger than the thermodynamic critical fields ($H_0\approx 1$ kG), in accord with the observations of Morin *et al.* (Ref. 68) on V_3 Ga. For $H=0$, $[C_{es}(T_c)/\gamma T_c]=2.4$ and $C_{es}/\gamma T_c=9\exp(-1.5\ T_c/T)$ in fair agreement with BCS (Ref. 28). For $H=4$ kG, $[C_{es}(T_s)/\gamma T_s]=1.9$ and $C_{es}/\gamma T_s=6\exp(-1.2T_s/T)$, $T_s(4\text{ kG})=3.4$°K, suggesting the presence of an essentially everywhere-finite high-field superconducting-state energy gap in accord with the Abrikosov (Ref. 9) vortex model.

[69] G. Bon Mardion, B. B. Goodman, and A. Lacaze, Phys. Letters **2**, 321 (1962).

[70] J. D. Livingston, Bull. Am. Phys. Soc. **7**, 534 (1962).

[71] B. B. Goodman, Phys. Letters **1**, 215 (1962).

[72] S. H. Autler, E. S. Rosenblum, and K. H. Gooen, Phys. Rev. Letters **9**, 489 (1962).

[73] P. S. Swartz, Phys. Rev. Letters **9**, 448 (1962).

[74] J. J. Hauser, Phys. Rev. Letters **9**, 423 (1962).

DeSorbo[75] for several transition metal alloys. Such measurements are of importance in further establishing the GLAG theory as a foundation upon which an understanding of *inhomogeneous* high-field superconductors may be constructed.

C. Transport Supercurrents and Inhomogeneities in Superconductors of the Second Kind

The regular lattice array of supercurrent vortices envisaged by Abrikosov does not correspond to a net macroscopic current flow (transport flow) in the interior of a superconductor of the second kind, nor did Abrikosov consider the influence of a transport current on the high-field superconducting state. Gor'kov[11] has argued that the GLAG-type high-field superconducting state is unstable with respect to a finite perturbation, and it has been speculated that the Lorentz forces associated with the net transport supercurrents may lead to instability of the high-field superconducting state in perfectly homogeneous superconductors.[19,20] We suggest that the experiments of Rose-Innes[76] may be interpreted as evidence in support of this viewpoint, for he observed that high-perfection alloy samples which exhibited nearly reversible Abrikosov-type (and, therefore, probably size-independent) magnetization curves were able to support only very small transport supercurrents at high fields. In any event, Abrikosov did suggest that inhomogeneities would be expected to modify the regularity of the lattice-like array of vortices in his theory and lead to a remnant moment as well. A magnetic-moment measurement would, in fact, be unable to distinguish between trapped Abrikosov-type flux-enclosing vortices and stabilized transport supercurrents of larger extent. Actually, transport supercurrent densities, typically $\sim 10^5$ A/cm^2, might be thought of as being superimposed upon the vortex supercurrent densities which are orders of magnitude greater. Such reasoning led to the conjecture[12,26] that vortex trapping might result in stabilization of a *transport-current-carrying*, GLAG-type, high-field superconducting state.

The condition for compensation of the Lorentz force in filamentary or laminar superconductors has been stated by Gorter[19,20] in terms of a spatial modulation of G_N-G_S [the free-energy difference, Eq. (2), between normal and superconducting states]. He also pointed out, as did Little,[77] that the requirements of flux quantization would also have to be satisfied in such a structure. Actually, the Lorentz force compensation mechanism is most likely equally applicable to the problem of transport supercurrent stabilization for a GLAG-type, high-field superconducting state, as was suggested by Anderson.[21] The latter author further considered the case of thermal activation of "flux bundles" (or vortices) over the modulations in G_N-G_S, thereby obtaining an expression for the temperature dependence of critical current density. Anderson's theory suggests that a spatial modulation of G_N-G_S amounting to $\sim 0.07\%$ over a distance of $\sim 10^{-5}$ cm would result in stabilization sufficient to account for the modest critical current densities observed by Kim *et al.*[78] in heat-treated Zr-75 Nb specimens.[79] Such a stabilization mechanism provides a natural explanation for the large anisotropies observed in the critical current densities of cold-rolled alloy superconductors[15–18,51] possessing highly anisotropic defect structures.[17,18] In such alloys, a maximum critical current density occurs for the case in which the Lorentz force is along a direction which micrographic examination[18] reveals as one of probable maximum free-energy modulation (viz., a direction perpendicular to the rolling plane). It is also significant that the Gorter-Anderson stabilization mechanism leads to the prediction of a hysteretic, size-dependent magnetization curve of the type[80] ordinarily observed for inhomogeneous superconductors of the second kind. It is important to emphasize at this point that the phenomenological magnetization curve equations of Bean[6] and of Kim *et al.*[78] (which describe such behavior) depend only on assumptions of particular functional relationships between *average* critical transport-current density and magnetic field strength and *are completely independent of* whether one assumes (1) a filamentary-mesh model (as they did in developing the phenomenological equations) or (2) the combinations of the GLAG theory and the Gorter-Anderson vortex stabilization mechanism. Thus, the assertion[74] that agreement between these phenomenological equations and experimental magnetization curves validates the filamentary-mesh model is incorrect.

In summary, the basis upon which an understanding of the majority of high-field superconductors may be built appears to be as follows. The GLAG theory and Clogston criterion predict an upper critical field at which superconductivity is quenched in the absence of transport supercurrent perturbations. This field is given in terms of the measurable bulk parameters ρ_n, γ, T_c, and S. At fields less than the upper critical field, the GLAG-type, high-field superconducting state can be destroyed by a critical transport-supercurrent density of magnitude determined principally (along the lines indicated theoretically by Gorter and Anderson) by the extent and nature of inhomogeneities. The inhomogeneously distributed transport supercurrent might be thought of as being superimposed on the spatially inhomogeneous vortex currents or as arising from gradients in the

[75] W. DeSorbo (private communication).

[76] A. C. Rose-Innes, remarks at the Eighth International Conference on Low-Temperature Physics, London, 1962 (unpublished).

[77] W. A. Little (private communication) (see also reference 17).

[78] Y. B. Kim, C. F. Hempstead, and A. R. Strnad, Phys. Rev. Letters 9, 306 (1962).

[79] It should be noted that in reference 21 an error amounting to a factor of 10 occurred in the numerical estimate for the fractional variation in G_N–G_S required to account for the results of Kim *et al.* (reference 78).

[80] Y. B. Kim, C. F. Hempstead, and A. R. Strnad (to be published).

strength and/or densities of vortices. The ability of a high-field superconductor to support transport supercurrents then goes hand in hand with its ability to exhibit irreversible, size-dependent magnetization characteristics.

D. Critique of the Filamentary-Mesh Model

As is evident from the foregoing, the characteristics of the majority of high-field superconductors can be accounted for in considerable detail without need for assumptions of the type introduced in the filamentary-mesh model.[1] Because this model has been extensively invoked in the scientific literature,[3–7,78] it is pertinent to tabulate experimental results which clearly contradict several of its features but are fully explicable on the basis of the picture which forms the central theme of this paper. The following remarks should *not*, however, be misconstrued to imply that an actual superconducting filamentary network cannot exist and exhibit the properties to be expected of such a structure.[1,6,78] The heterogeneous Hg and vycor samples fabricated by Bean *et al.*[81] are obvious examples, and incompletely sintered Nb-Sn complexes might be inhomogeneous enough to qualify as filamentary-mesh superconductors. Thus, the comments below are intended only to indicate where flaws exist in some of the concepts, features, and extensions of the filamentary-mesh model, and to emphasize how restricted is its realm of applicability.

Considerable confusion is evident in the literature as a consequence of the rather common assumption (relative to the filamentary-mesh model) that the change in an experimental quantity (such as, for example, the magnetization or critical current density) necessarily represents a corresponding change in the *volume* of superconducting material. Viewed in terms of the GLAG theory, a property change is, in general, interpreted as a change in some complicated spatial average $\langle\omega\rangle$ of the order parameter. It is predicted that $\langle\omega\rangle$ will go to zero continuously (second-order transition) as $T\rightarrow T_c$ or $H\rightarrow H_{c2}$. (The case $J\rightarrow J_c$ is complicated by the considerations already discussed.) Even though $\langle\omega\rangle$ (or, for example, the magnetization) may be very close to zero, the entire volume of a superconductor of the second kind remains superconducting in the sense that $\omega>0$ everywhere except along a line at the center of each vortex.

The high upper critical fields of high-field superconductors have been attributed on the filamentary-mesh model to the small *dimensions* of multiply connected filamentary regions which are *assumed* to exist.[3–5] As discussed above, such a concept is superfluous for a system in which a high upper critical field is already assured by a large κ value.

Several predictions follow from the assumption[1] of a high-critical-field filamentary network embedded in a low-critical-field matrix. If filaments are attributed to a particular type of inhomogeneity (such as, for example, a dislocation) the magnetization curve should change quasicontinuously with increasing inhomogeneity concentration from that characteristic of an ideal (first group) superconductor to that characterized by the phenomenological equations of Kim *et al.*[78] In other words, *the filamentary-mesh model predicts that* (1) flux penetration will commence at a field equal to or greater than (but never less than) the thermodynamic critical field and (2) any specimen exhibiting a measurable superconducting moment in fields greater than the thermodynamic critical field will exhibit an appreciable hysteresis. These predictions are flatly contradicted by (1) the observed flux penetration for fields much less than H_c in both homogeneous and inhomogeneous superconductors of the second kind[58–60,69,70,73,74] and (2) the observed near approach to reversibility in the magnetization curves of homogeneous superconductors of the second kind.[60,69,70] Both of these experimental results are in good accord with the GLAG theory.

In extensions of the filamentary-mesh model, a filamentary critical field H_f has been assumed to be associated with material in the vicinity of a dislocation, and it has been further assumed that H_f is approximately the same for every filament.[4] Accordingly, the vanishing-current-density resistive critical field of a perfect single crystal of Nb, for example, would increase from H_c to H_f with the introduction of a single dislocation and would then remain unchanged as more dislocations are added. However, experiments[58,72] noted above suggest that an upper critical field greater than H_c is an inherent characteristic of defect-free Nb. Furthermore, in contrast to the case for concentrated alloys of the type studied in the present investigation, ρ_n for pure Nb is strongly dependent upon dislocation content (or cold working), and, as a consequence, the upper critical field is also.[50] The relatively broad transitions observed[50] for cold-worked Nb suggest that work-induced defects are inhomogeneously distributed, leading to a position-dependent κ. For this reason, quantitative agreement in this case would hardly be expected (nor is it obtained[82]) between experiment and values of H_{c2} calculated using bulk resistivity values in the GLAG equations. Actually, such a system appears to possess some (though clearly not all) of the characteristics predicted by the filamentary-mesh model.

Perhaps the most difficult experimental result to rationalize in terms of the filamentary-mesh model is the bulk nature of the calorimetrically observed super-

[81] C. P. Bean, M. V. Doyle, and A. G. Pincus, Phys. Rev. Letters 9, 93 (1962).

[82] The low-current-density resistive critical fields for high-purity cold-worked Nb samples (reference 50) exceed values of H_{c2} calculated using bulk resistivity data, whereas the opposite result is obtained for annealed impure samples (reference 72). The former result could arise if the resistivity in the vicinity of highly deformed (dislocation-saturated) regions exceeds the average resistivity. The impure sample result may arise either from homogeneous chemical contamination or from segregation of impurities near dislocations, since either of these possibilities could reduce γ and/or T_c enough to yield the observed results.

conducting transition in high magnetic fields. If, as indicated by the measurements of Morin *et al.*,[68] $\frac{7}{8}$ of the electronic assembly in V_3Ga is in the superconducting state in a field of 70 kG, it is not appropriate to describe the system as being comprised of a filamentary superconducting network, occupying $\frac{7}{8}$ of the volume, embedded in a normal state matrix, occupying $\frac{1}{8}$ of the volume.

On the positive side, one may speculate that the filamentary-mesh model might be approximately appropriate for a specimen comprised mainly of material which is inherently of the first kind, but, by reason of inhomogeneously distributed impurities or strains, may possess a filamentary network for which $\kappa<1/\sqrt{2}$. Such may actually have been the case for the specimens studied by Shaw and Mapother.[83]

E. Some Remaining Problems

Despite the considerable successes of the GLAG–Clogston and Gorter–Anderson theories discussed in this paper, a number of unanswered questions remain. Perhaps some of the most puzzling aspects of high-field superconductors are to be found in the interrelated maxima (peak effects) which occur in (1) the critical current density as a function of magnetic field[15,16,18,84] (see Fig. 10), (2) the critical current density as a function of temperature,[72,85] and (3) the resistivity as a function of magnetic field.[50,51] Such effects are not explicitly accounted for by the Gorter-Anderson Lorentz force–thermal activation ideas, although extensions of this formalism to take explicit account of the relative spacings of the Abrikosov-type vortices and a characteristic defect structure (e.g., dislocation network spacing) might conceivably contribute to an understanding of these phenomena.[26]

Of great interest would be high-magnetic-field, low-temperature specific heat measurements on an inhomogeneous second-group superconductor *carrying a large transport supercurrent density*. The interest in this particular experiment centers on the (possibly unique) ability of a specific heat measurement to assess quantitatively the relative volumes of superconducting and normal material, and the question of whether or not large transport supercurrents might shrink the volume of superconducting material appreciably. Such a measurement could probably be accomplished by cooling a cylindrical shell specimen in a high magnetic field and then inducing a high transport-supercurrent density by reducing the applied field a small amount.

Comparisons between H_{c2} and the low-current-density resistive critical field were not possible for the majority of the alloys studied in this investigation simply because of lack of data on γ. Such data would thus be of value in permitting a more complete test of the GLAG theory.

The importance of experimental determinations of H_{c1} for Ti-V alloys (for comparison with the theoretically predicted values in Fig. 20) has already been mentioned as a worthy test of the GLAG theory for a field range in which normal-state paramagnetic free-energy terms should be unimportant. Good agreement would strengthen the belief that the discrepancy between H_{c2} and $H_r(J=10)$ for alloys such as Ti-50 V is truly attributable to limitations imposed by the Clogston criterion. Of interest in this same connection would be a theoretical investigation of the consequences of introduction of normal-state paramagnetic free-energy terms into the beginning of the GLAG theory. Such a theory would substitute a single, more meaningful comparison for the piecemeal comparison of $H_r(J=10)$ with both H_{c2} and H_p in this investigation. A more ambitious theoretical program might even consider the consequences of the simultaneous introduction of a transport current *and* a spatial modulation of G_N-G_S into the GLAG theory.

Finally, the successes of the GLAG theory would appear to justify rather elaborate attempts to "observe" the vortex lattice in homogeneous superconductors of the second kind. On the surface it would appear that, by virtue of the electromagnetic nature of supercurrent vortices, experimental tests of their existence might be more easily accomplished than tests of the existence of the elusive superfluid vortices purported to exist in liquid helium II.[86] It is, of course, possible that some other negative-surface-energy structure might possess a lower energy than that characteristic of Abrikosov's "square" vortex lattice.

ACKNOWLEDGMENTS

It is a pleasure to acknowledge D. H. Leslie for assistance with the measurements, D. M. Sellman for sample preparation, and D. G. Swarthout for x-ray analyses. We are indebted to J. Wong of the Wah Chang Corporation for several wire samples of Ti-Nb and Zr-Nb alloys, and R. D. Blaugher and W. C. H. Joiner of the Westinghouse Research Laboratories for the transition temperature data on Ti-Ta alloys.

[83] R. W. Shaw and D. E. Mapother, Phys. Rev. **118**, 1474 (1960).

[84] M. A. R. LeBlanc and W. A. Little, in *Proceedings of the Seventh International Conference on Low-Temperature Physics*, edited by G. M. Graham and A. C. Hollis Hallet (University of Toronto Press, Toronto, 1961), p. 362.

[85] R. R. Hake, remarks at Eighth International Conference on Low-Temperature Physics, London, 1962 (unpublished).

[86] For a review of theory and experiment, see W. F. Vinen, in *Progress in Low-Temperature Physics*, edited by C. J. Gorter (Interscience Publishers, Inc., New York, 1961), Vol. III, p. 1 ff.

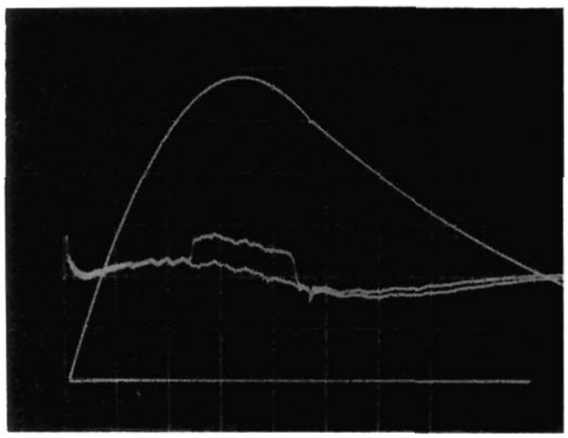

FIG. 2. Oscilloscope recording of magnetic-field-induced resistive transitions for Ti-28.7 V at 1.2°K with $H \perp J$ and $H \| RP$. The wiggly traces represent the signal (1 mV/cm) on the potential probes for two successive (and indistinguishable) magnetic-field pulses with and without a measuring current density of $J=10$ A/cm². The magnetic field is shown rising from zero to 107 kG in 6.6 msec.